Long Range Prediction of Fading Signals: Enabling Adaptive Transmission for Mobile Radio Channels[1]

Alexandra Duel-Hallen[+], Shengquan Hu[+], Hans Hallen[*]

[+]North Carolina State University
Dept. of Electrical and Computer Engineering
Center for Advanced Computing and Communication
Box 7914, Raleigh, NC 27695-7914
E-mail: sasha@eos.ncsu.edu, shu@eos.ncsu.edu

[*]North Carolina State University
Physics Department
Box 8202, Raleigh, NC 27695-8202
E-mail: Hans_Hallen@ncsu.edu

ABSTRACT

Recently it was proposed to adapt several transmission methods, including modulation, power control, channel coding and antenna diversity to rapidly time variant fading channel conditions. Prediction of the channel coefficients several tens-to-hundreds of symbols ahead is essential to realize these methods in practice. We describe a novel adaptive long range fading channel prediction algorithm (LRP) and its utilization with adaptive transmission methods. This channel prediction algorithm computes the linear Minimum Mean Squared Error (MMSE) estimates of future fading coefficients based on past observations. This algorithm can forecast fading signals far into the future due to its significant memory span, achieved by using a sufficiently low sampling rate for a given fixed filter size. The LRP is validated for standard stationary fading models, and tested with measured data and with data produced by our novel realistic physical channel model. This model accounts for the variation of the amplitude, frequency and phase of each reflected component of the fading signal. Both numerical and simulation results show that long range prediction makes adaptive transmission techniques feasible for mobile radio channels.

Key words: — adaptive long range fading channel prediction, adaptive modulation, adaptive power control, adaptive coding, transmitter diversity, Rayleigh fading channel, realistic physical modeling.

1. INTRODUCTION

The 3rd generation of wireless systems is endeavoring to satisfy growing consumer demands [1, 2]: transmitting high-speed data (up to 2Mbits/s), video, multimedia traffic as well as voice signals to mobile users. This tremendous growth in demand for wireless communications capacity has created a need for

[1] This work was supported by NSF grants CCR-9725271 and CCR-9815002.

new modulation, coding, power control and detection methods that can more efficiently use the multipath fading channels encountered in mobile radio. However, since the channel changes rapidly, the transmitter and receiver are not usually optimized for current channel conditions, and thus fail to exploit the full potential of the wireless channel. Recently, several new *adaptive transmission techniques*, such as adaptive modulation [3 - 22], adaptive channel coding [23 - 31], adaptive power control [4, 25, 26], and adaptive transmitter antenna diversity [32 - 36], have been investigated by many researchers. These adaptive transmission schemes vary the constellation size, symbol rate, coding rate, transmitted power level, weights of transmission antennas, or any combination of these parameters by instantaneously monitoring channel conditions. Other recently proposed adaptive transmission techniques include adaptive processing gain and frame length control [37, 38] for Direct Sequence Code Division Multiple Access (DS/CDMA) systems, as well as adaptive quantizer designed to match fading channel states [39]. By taking advantage of the time-varying nature of the wireless fading channel, all these adaptive schemes are trying to use both power and spectrum more efficiently to realize the higher bit rate transmission without sacrificing the Bit Error Rate (BER) performance. It is anticipated that adaptive transmission methods will be utilized in many wireless products in the near future. As an example, the 3rd generation GSM phase 2+ system expected on the market by the year 2000 utilizes Adaptive Multi Rate codec (AMR) to further improve GSM speech service [40].

To implement adaptive transmission methods in practice, the *channel state information* (CSI) must be available at the transmitter. CSI can be estimated at the receiver and sent to the transmitter via a feedback channel. Thus, feedback delay and overhead, processing delay and practical constraints on modulation, coding and/or antenna switching rates have to be taken into account in the performance analysis of adaptive transmission methods. For very slowly fading channels (pedestrian or low vehicle speeds), *outdated* CSI is sufficient for reliable adaptive system design. However, for faster fading that corresponds to realistic mobile speeds, even small delay will cause significant degradation of performance since channel variation due to large Doppler shifts usually results in a different channel at the time of transmission than at the time of channel estimation [4, 22, 56]. To realize the potential of adaptive transmission methods, these channel variations have to be *reliably predicted* at least several milliseconds, or tens to hundreds of data symbols ahead.

While many researchers have addressed a related problem of estimation of current fading conditions, prediction of future fading coefficients has not been addressed until recently. While most of this paper focuses on our long range prediction algorithm [49 - 59], some other prediction methods proposed in the literature are summarized below. In [41], an ESPRIT-type algorithm was used to estimate the dominant sinusoids that make up the fading signal. Then these sinusoids were extrapolated to predict future samples. Both synthetic and real data was examined, and it was concluded that reliable prediction is

feasible about a wavelength ahead (or 10 ms ahead for the vehicle speed of 68 miles per hour and the carrier frequency of 1 GHz). Since fades occur at least half a wavelength apart, this prediction capability means that a future deep fade can often be forecasted. In [42], Multivariate Adaptive Regression Splines (MARS) model was used to predict parameters of wideband fading channels several milliseconds ahead for fast vehicle speeds, and information-theoretical analysis was performed to demonstrate the long-range prediction capability. Obviously, the required prediction range is dictated by the application, and in many instances (e.g., selection of RAKE fingers or of the receiver antenna), prediction only a few data symbols to a millisecond ahead is satisfactory. Several methods have been reported in the literature to achieve reliable prediction performance in this range for mobile radio channels. Examples of these investigations include the root-MUSIC methods [43], neural network based predictors [44], nonlinear Volterra adaptive prediction [45], and Prony algorithm based channel prediction [46]. In addition, the authors of [47] introduced prediction of channel state for the Finite State Markov Channel (FSMC) [48] employed in conjunction with an adaptive modulation/coding study [24].

To achieve desired long range prediction capability, the above methods require a long observation interval and heavy computational load to compute current model parameters. In rapidly changing mobile radio environments, the vehicle speed and scattering geometry change continuously, and thus the model parameters need to be recomputed frequently. Thus, there is a need for *adaptive low complexity* long range prediction techniques that meet the accuracy requirements of adaptive transmission schemes for realistic mobile radio channels.

We have investigated a *novel adaptive long range fading channel prediction algorithm (LRP)* in [49 - 59]. This algorithm characterizes the fading channel using an autoregressive (AR) model and computes the Minimum Mean Squared Error (MMSE) estimate of a future fading coefficient sample based on a number of past observations. The superior performance of this algorithm relative to conventional methods is due to its *low sampling rate* (on the order of twice the maximum Doppler shift and much lower than the data rate) [52, 53]. Given a *fixed model order*, the lower rate results in *longer memory span*, permitting prediction further into the future. The prediction method is enhanced by an *adaptive tracking* method [52, 53] that increases accuracy, reduces the effect of noise and maintains the robustness of long range prediction as the physical channel parameters vary. In addition to testing our method on standard stationary fading models [49, 51 - 53], we utilize a method of images to create a novel physical channel model where fading is viewed as a deterministic process formed by the addition of several scattered components [54, 58]. The amplitude, frequency and phase of each component slowly vary as the vehicle moves through an interference pattern. The variation of these parameters is not captured by the standard Jakes model [60] or a stationary random process description [61]. However, the accuracy of the LRP is determined by the rate of change of these parameters. The novel physical model allows us to

test the proposed LRP algorithm and identify typical and challenging situations encountered in practice. We also use field measurements provided by Ericsson, Inc. to validate the performance of our prediction method and the insights of the novel physical model [54, 55, 58]. Finally, power prediction for wideband CDMA (WCDMA) was addressed in [56].

The goal of the LRP method is to enable adaptive transmission. In [50 - 53, 55, 58, 59], we have combined LRP with the truncated channel inversion power control method [4, 62]. In [57], joint adaptive variable rate Multilevel Quadrature Amplitude Modulation (MQAM) [4] and LRP was addressed. Combined long range power prediction and Selective Transmission antenna diversity (STD) [36] for WCDMA was studied in [54].

In this paper, we summarize these findings and quantify performance gains achieved when future fading estimates produced by the LRP are used instead of the outdated CSI. The paper is organized as follows. In section 2, we review fading channel models and adaptive transmission methods and discuss the importance of accurate long range channel prediction in adaptive transmission. We describe the LRP algorithm and its utilization in conjunction with adaptive modulation in section 3. Finally, in Section 4, our novel physical model is discussed, and results of testing the performance of the LRP on the interference patterns created using this model and on measured field data are presented.

2. ADAPTIVE TRANSMISSION FOR FADING MOBILE RADIO CHANNELS

Characterization of Fading Channels

In wireless communication systems, the received signal experiences significant power fluctuations due to fading [60, 61, 63 - 65]. Signal fading is caused by multipath propagation and Doppler frequency shift. Multiple scatterers give rise to multipath that causes interference between reflected transmitter signal components. As the mobile drives through this interference pattern, a typical fading signal results as illustrated in Figure 1. The superposition of component waves leads to either constructive (*peaks*) or destructive interference (*deep fades*). When all delayed components arrive at the receiver within a small fraction of the symbol duration, the fading channel is *frequency-nonselective,* or *flat*. This often occurs in *narrowband* signaling. In *wideband* transmission, the *multipath delay* is often non-negligible relative to the symbol interval, and *frequency-selective* fading results. In addition, when the receiver, the transmitter, and/or the scatterers are moving, the n-th *scattered component* undergoes a *Doppler frequency shift* given approximately by [65]:

$$f_n = f_c \frac{v}{c} \cos\theta_n = f_{dm} \cos\theta_n \qquad (1)$$

where f_c is the carrier frequency, v is the vehicle speed, c is the speed of light, θ_n is the incident radiowave angle with respect to the motion of the mobile, and f_{dm} is the *maximum Doppler frequency shift*. The complex envelope of the flat fading signal at the receiver is

$$c(t) = \sum_{n=1}^{N} A_n \, e^{\,j(2\pi f_n t + \phi_n)}, \qquad (2)$$

where N is the number of scatterers, and for the n^{th} scatterer, A_n is the amplitude, f_n is the Doppler frequency shift in (1), and ϕ_n is the phase. The parameters A_n, f_n, and ϕ_n are *slowly time-variant* as discussed later in the paper. Throughout the paper we assume without loss of generality that the average channel power $E(|c(t)|^2)$ is normalized to one. This standard assumption simplifies performance analysis and is not used in channel estimation and prediction. A fading channel is often called *rapidly time-varying*[2] when a mobile passes through several fades in a second [66]. Faster vehicle speeds and larger carrier frequencies cause more rapid fluctuations in the fading signal.

A well known statistical model that characterizes a flat fading channel without the *Line of Sight* (LOS) is *Rayleigh fading* in which the fading coefficients are modeled as the complex Gaussian random variables [60, 61]. A deterministic *Jakes model* [60] is used as a standard model in computer simulations. Using Jakes model, the theoretical Doppler spectrum of the Rayleigh fading channel can be accurately approximated by a summation of a relatively small number of sinusoids (usually less than nine) [60]. The sinusoidal signal decomposition (2) was utilized in channel estimation methods [84, 86 - 88] and several channel prediction methods reviewed in Section 1.

Adaptive Transmission Techniques

In contrast to the additive white Gaussian noise (AWGN) channel characterized by a constant signal Signal-to-Noise ratio (SNR), in mobile radio channels the SNR is time-variant due to multipath fading and interference from other users. In this paper we model the multiuser interference as additive Gaussian noise, and focus on *transmission techniques that combat channel fading*. Conventional constant transmitted power and bit rate design suffers severe performance penalty due to the Bit Error Rate (BER) degradation during deep fades when the channel power is very low [61]. This results in high transmitted power requirements. For example, the Binary Phase Shift Keying (BPSK) in Rayleigh fading requires the transmitted SNR=24 dB to achieve the BER = 10^{-3}. Using adaptive power control, the transmitted power can be allocated according to the instantaneous channel strength. For example, in the truncated channel inversion method (TCI) [4, 51, 52], transmission is avoided when the instantaneous channel power falls below a certain threshold (during deep fades), and the transmitted power is proportional to the inverse of the fading channel power when it is above the threshold. Assuming perfect CSI at the transmitter, the

[2] This is different from the definition of fast fading where channel variation is at the symbol rate [63, 65].

BER=10^{-3} can be achieved by TCI when the average transmitted SNR = 7dB and the threshold = 0.4. This matches the performance of the AWGN channel. For higher thresholds, TCI is even more energy efficient since the channel is used only when it is very strong. (Due to constructive interference, the power of the peaks in the fading channel (Fig. 1) exceeds that of the AWGN channel.) In Section 4, we remove the perfect CSI assumption and combine TCI with our LRP method (see Figure 10).

TCI is not a practical method since it requires rapid transmitted power variation. In addition, its performance improvement is achieved at the expense of lower normalized data rate (bandwidth efficiency), since the data is not transmitted when the fading level is below the threshold. Bandwidth and power efficient adaptive modulation can be achieved by varying the constellation size M (and therefore bit rate) according to channel strength. For fixed bandwidth, larger values of M result in higher bit rates, but also have higher SNR requirements [61]. In adaptive methods, higher M are chosen when the channel is strong, and extra power is available, and lower M are reserved for poor channel conditions [67, 68]. Bandwidth and power gains of these methods are due to two important properties: first, constant power and modulation size techniques suffer most BER degradation during deep fades; and second, the fading channel spends most of the time outside deep fades (Figure 1). Thus, adaptive modulation techniques use relatively high average constellation size (and bit rate) most of the time, and avoid severe BER penalty by reducing the bit rate and using power efficient low modulation sizes (or turning off transmission entirely) during deep fades. Thus, the transmission load is shifted away from the deep fades and increases as the channel gets stronger. As a result, much faster bit rates relative to non-adaptive techniques can be achieved without sacrificing the BER performance [4]. For example, consider the following simple adaptive modulation scheme: when the amplitude of the normalized channel coefficient is greater than an appropriately chosen constant threshold, 16-QAM is used for the transmission, otherwise, 4-QAM is used. The simulation result for the threshold of 0.3 is shown in Figure 2. In this figure, it is assumed that perfect CSI is available at the transmitter. We observe that the adaptive modulation scheme retains most of the bandwidth efficiency of 16-QAM, while matching or surpassing the energy efficiency of the conventional 4-QAM.

Overview of adaptive transmission methods

Variable constellation size signaling strategy was proposed in [69 - 71] and have been successfully used in the V. 34 telephone modem [72]. More recently, adaptive modulation for mobile radio channels has attracted substantial research interest [3 - 22, 28, 73 - 75]. Most of this research work focuses on the following issues: modulation level selection rule [4, 10, 12, 13, 21, 22], transmit signal power control policy [4, 73], symbol rate switching criteria [10, 28], classification of the demodulation level [9, 17], channel estimation and prediction [10, 28], the effect of channel estimation errors, feedback delay and mobile speed [4, 10], and the performance analysis of throughput and BER [4, 10, 15, 74]. The

performance of adaptive modulation schemes can be further improved when antenna diversity is used at the receiver [7]. Hardware constraints on the implementation of adaptive modulation were considered in [75].

Accurate prediction of future CSI is essential for implementation of the adaptive modulation algorithms, and several researchers considered this problem. For example, adaptive modulation design aided by predicted CSI was considered in [10, 28]. However, either short range prediction or very slow fading were addressed in these investigations. Adaptive signal design using delayed fading estimates was studied in [21]. In that paper, the current channel fading amplitude conditioned on the delayed fading estimates is characterized as a Rician random variable, and the design requires the knowledge of the correlation coefficient between the current channel state information (CSI) and the outdated fading estimates. In practice, the autocorrelation function is generally not known at the transmitter. Moreover, with this design rule even very small delays cause significant bit rate loss (e.g. 0.8ms delay for Maximum Doppler shift 100Hz corresponds to correlation coefficient $\rho = 0.94$ in [21] which causes at least 1bit/symbol bit rate loss relative to the ideal case).

In mobile radio environment, it is also often of interest to consider *adaptive channel coding* techniques that conserve power (see [62, 76]). An efficient approach is to vary the code rate according to the fading channel conditions [23, 24, 26, 77]. The basic idea is to select a code with low rate when the channel is going into a fade, and a high rate code when the channel becomes stronger. For example, BCH codes with several different rates were used in [24, 26] and an adaptive Reed-Solomon code in [77]. Punctured convolutional codes were utilized in [23] since they have superior performance and availability of a wide range of code rates without changing the basic structure of the encoder and decoder (codec).

Recently, *adaptive trellis coded modulation* (TCM) methods that provide both power and bandwidth efficiency have been investigated in, e.g. [3, 23, 29, 73, 77 - 80]. For example, the theoretical and simulation results in [3] showed that 3-dB and 4-dB gain relative to uncoded adaptive modulation can be achieved by a four- and eight- state adaptive TCM, respectively.

Adaptive transmission for antenna array systems has also attracted the attention of researchers. Diversity antenna arrays require several antenna elements placed with sufficient separation at the transmitter and/or the receiver. As with temporal or frequency diversity methods, they help to combat fading by resolving several fully or partially decorrelated fading channels. Since it is unlikely that these channels will go through a deep fade at the same time, higher average received SNR results when the outputs of the branches are combined. Many recent investigations focused on transmitter diversity techniques for the downlink since, in practice, a mobile is often limited to a single antenna, while a base station can employ several antennas. Those transmission diversity techniques that do not utilize CSI at

the transmitter can be classified as non-adaptive. We focus on adaptive transmission diversity methods that usually require feedback from the receiver to the transmitter, but also have better performance than non-adaptive techniques (see [32, 56].) In fact, it can be shown that, assuming perfect CSI, there is no BER loss due to placing multiple antennas at the transmitter rather than at the receiver. For example, the Transmitter Adaptive Array method (TxAA) [32] is equivalent to the Maximal Ratio Combining (MRC) at the receiver [61], while Selective Transmitter Diversity (STD) [33, 36] matches the performance of selection diversity for the receiver array. Due to its implementation simplicity, the STD scheme has attracted significant interest recently. In the STD the channel power of each transmitter antenna is monitored at the receiver, and the antenna with the strongest power is selected for transmission.

The importance of long range channel prediction in adaptive transmission

As we discussed in the introduction, accurate knowledge of future CSI is extremely important for realizing the potential of adaptive transmission. As an example, consider the application of STD in the proposed 3rd generation WCDMA system [81, 82]. One of the key features that makes WCDMA feasible globally is its high carrier frequency of 2 GHz. However, this high carrier frequency results in very large Doppler shifts at moderate vehicular speeds (e.g. 65 mi/h corresponds to f_{dm}= 200 Hz) that cause significant variations of the fading channel coefficients over short time periods. Thus, outdated channel estimates fed back to the transmitter become less useful for adaptive signaling application, and long-range fading prediction capability becomes more important [56]. For example, in Figure 3, we compared the BER performance of the STD scheme with and without channel prediction for two transmitter antennas that are separated sufficiently far apart that the signals transmitted from these antennas experience independent flat Rayleigh fading (similar results were obtained for multipath fading). Based on the received power, the strongest antenna is selected at the receiver. The antenna selection bit is sent back to the transmitter and determines the antenna that is going to transmit during the next slot (switch at 1.6KHz curves) or during the next four slots (switch at 400Hz curves.) For STD without prediction, this bit is based on the power of the noiseless pilot symbol received in the last slot. Thus, the CSI is delayed by the slot duration (0.625ms) relative to the beginning of the switching interval. When long range prediction is utilized, previous noiseless pilot symbols collected at the rate of 1.6KHz are used to predict the average channel power during the next switching interval. The most recent observation is also delayed by 0.625ms with respect to the antenna selection instance. This predicted power determines the value of the antenna selection bit. Results show that significant performance gains (here around 4dB) are achieved for fast vehicle speeds when LRP is employed. As described below, comparable or greater gains are also possible for other adaptive transmission techniques using long range prediction.

3. LONG RANGE PREDICTION OF RAPIDLY VARYING FADING CHANNELS

The MMSE prediction of the flat fading channel using the AR model

The objective of the long-range prediction is to forecast future values of the fading coefficient far ahead. To accomplish this task, a linear prediction (LP) method based on the AR modeling was proposed in [49, 51]. Consider the equivalent lowpass discrete-time system model at the output of the matched filter and sampler given by:

$$y_k = c_k\, b_k + z_k, \tag{3}$$

where c_k is the flat fading signal sampled at the symbol rate, b_k is the binary phase shift keying (BPSK) data sequence, and z_k is the complex discrete AWGN process with the variance $N_0/2$. Suppose a sequence of p previous samples of the fading signal is observed. (In general, the sampling rate differs from the data rate. Throughout this paper, the subscript n refers to the sampling rate for prediction purposes, and k to the data rate.) The MMSE prediction of the future channel sample $\hat{c}_n$ based on p previous samples c_{n-1}, ... , c_{n-p} is given by:

$$\hat{c}_n = \sum_{j=1}^{p} d_j c_{n-j} \tag{4}$$

where p is the AR model order, and the optimal coefficients d_j are determined by the orthogonality principle [83] as:

$$\underline{d} = \underline{R}^{-1}\, \underline{r}, \tag{5}$$

where $\underline{d} = (d_1,\cdots,d_p)^T$, $\underline{R}$ is the autocorrelation matrix (p×p) with coefficients $R_{ij} = E[c_{n-i}\, c^*_{n-j}]$ and $\underline{r}$ is the autocorrelation vector (p×1) with the coefficients $r_j = E[c_n\, c^*_{n-j}]$. The correlation coefficients R_{ij} and r_j can be estimated from the observation samples without the prior knowledge of the Maximum Doppler shift or the number of scatterers. Note that the samples in (4) have to be taken at least at the Nyquist rate given by twice the maximum Doppler frequency f_{dm}. The sampling rate we choose is close to this Nyquist rate and therefore is much lower than the data rate in (3). The predicted samples can be interpolated to forecast the fading signal at the data rate [49 - 51].

To show that the lower rate sampling can result in more accurate long range prediction when the filter length p in (4) is fixed, we extend one-step prediction in (4) to a general channel prediction problem as follows. The objective is to find the MMSE estimate of a future sample $c(\tau)$ $(\tau > 0)$ by observing p previous samples collected at and prior to time zero at the sampling rate $f_s = 1/T_s$. The predicted value:

$$\hat{c}(\tau) = \hat{c}_\upsilon = \sum_{j=0}^{p-1} d_j c_{-j} \tag{6}$$

The interval $\tau = \upsilon T_s$ is called the prediction range, where υ can be any positive real number [3]. The LP filter coefficients d_j can be determined as in (5) by minimizing the MSE, $E[|e(\tau)|^2]=E[|c(\tau) - \hat{c}(\tau)|^2]$. The resulting MMSE is given by:

$$E[|e(\tau)|^2] = 1 - \sum_{j=0}^{p-1} d_j r(\tau+jT_s), \tag{7}$$

where the autocorrelation function $r(t)= E[c(s)c^*(s+t)]$. For the Rayleigh fading channel (throughout the paper, when we refer to Rayleigh fading, we assume isotropic scattering environment [60]):

$$r(t) = J_0(2\pi f_{dm} t) \tag{8}$$

where $J_0(.)$ is the zero-order Bessel function of the first kind [60]. The plot of this function is shown in Figure 4 for f_{dm} = 100 Hz. For given model order p and sampling rate f_s, we define the memory span as: $(p-1) \times Ts = (p-1)/f_s$ which measures the observation interval used in (4, 6) for the future channel coefficient prediction. Now, let us discuss how the memory span is related to the performance of the MMSE channel prediction. Fix model order p, and vary the sampling rate f_s. As f_s increases, the portion of the autocorrelation function spanned by the samples $r(\tau+jT_s)$ in (7) decreases. For example, in Fig. 4, for p = 20, f_s = 25 kHz results in a memory span of only 0.76 ms when f_{dm}=100Hz. The range of values of the autocorrelation function samples along this interval is small. When we try to predict channel far ahead, i.e. when τ is large (see Fig. 4), these autocorrelation values become small, and the MMSE (7) increases. Now, let us consider prediction at a lower sampling rate. In this case, the observation samples are spaced much further apart and result in a large memory span (in Fig. 4, when p = 20 and f_s = 500 Hz, the memory span becomes 38 ms). The autocorrelation values used in (7) significantly vary over this interval for any realistic prediction range. Due to the large sidelobes of the autocorrelation function, some of these autocorrelation samples are large enough to keep the MMSE from getting very large, and reliable long range prediction can be achieved even when the prediction range is much greater than conventionally defined coherence time[4] [65].

The effect of the sampling rate was evaluated in [53], and it was found that for each model order p there is an optimal low sampling rate that minimizes the MMSE. Given the maximum Doppler shift of 100Hz, for the Rayleigh fading channel (characterized by the infinite number of scatterers) this optimal rate is close to 1KHz for moderate to high model order p ($p \geq 10$). In practice, the number of effective scatterers is usually modest (usually not more than 20), and the sampling rate of 500 Hz gives the best performance [53]. Note that when noisy observation are used in (7), the effect of the noise is incorporated into $\underline{R}$ in (5) by adding $(N_0/2)\underline{I}$ where $\underline{I}$ is the p×p identity matrix. While $\underline{R}$ can be singular in the noiseless

[3] When τ is an integer multiple of the sampling interval, i.e., $\tau = \upsilon T_s$ where υ is an integer, we call this υ-step prediction.

[4] In this paper, the coherence time τ_0 corresponds to $r(\tau_0)=1/2$, where r(.) is the autocorrelation function of a given fading process [65].

case due to the oversampling relative to the Nyquist rate (=$2f_{dm}$)[56], the inverse in (5) can usually be computed when additive noise is present. The theoretical performance comparison of the MMSE performance of the long range prediction with various sampling rates is shown in Figure 5. For example, when f_{dm}=100 Hz, the range of 0.2 on the x-axis corresponds to 2 ms, or 50 data symbols ahead assuming the sampling rate given by the data rate of 25 kHz, and 1 sampling point ahead with a lower sampling rate of 500 Hz. As seen from the figure, the same future value can be predicted with much greater accuracy by using the low sampling rates. Thus, when the sampling rate is reduced greatly relative to the data rate, but the filter length p remains the same, prediction much further ahead becomes feasible.

In the discussion above, the complex-valued flat fading coefficients are predicted and observed. However, in some cases, prediction of the channel power is of interest. For example, in the decision directed channel estimation, phase ambiguity makes prediction of future complex values problematic. But this is not a serious limitation, since implementation of many proposed adaptive transmission techniques, e.g. [4], depends on the knowledge of future power only, and phase prediction is not necessary. Furthermore, for frequency-selective channels future total channel power can be utilized in adaptive transmission. For example, in the investigation of selection transmitter diversity study for WCDMA, we utilized predicted total channel power obtained from the outputs of the RAKE receiver [56]. In the prediction of fading power, increased memory span also insures large prediction range required for adaptive transmission applications.

Adaptive long range prediction

In practice, many factors affect the performance of the long range prediction. First, the autocorrelation function of the channel is not known a priori. To compute the initial estimates of the channel coefficients $\underline{d}$ as in (5), we utilize an observation interval that consists of a number of received channel samples. When this interval is not sufficiently long, the LRP suffers degradation due to the model mismatch. This mismatch is further enhanced by channel variation due to changes in the vehicle speed and positions of the scatterers. Accurate prediction is also affected by additive noise and data-dependent observations (unless pilot signals are used). Finally, when the prediction interval is longer than one step ahead (multi-step prediction), we iterate the equation (4) by using previously predicted samples instead of the observations. This can result in error propagation.

Below we describe several techniques that can be used to improve prediction accuracy. Since these methods involve adaptive tracking, we refer to the resulting algorithms as *adaptive long range prediction*. Throughout this section, we use the flat Rayleigh fading random process in all theoretical results and the standard Jakes model [60] in all the simulations. Unless specifically noted, we assume that the Jakes model has nine oscillators, and the maximum Doppler frequency shift is 100 Hz.

Consider first the problem of predicting one step ahead (as in (4)), but using the samples of the received signal y_k (3) at the data rate to estimate the observations c_n at the low sampling rate. Assuming that the data rate is 25Kb/s, and the sampling rate is 500Hz, this results in the prediction of 2ms or 50 bits ahead. Since the data bits are not known a priori, either training bits or decisions can be used in this estimation process. In the results below, we assume that correct decisions are available, and let the received samples be $y_k = c_k + z_k$. To obtain the estimates of c_n, one can simply use the noisy observations y_n collected at the low sampling rate. However, at low SNR, this results in unacceptable degradation of prediction accuracy. Instead standard estimation procedures can be utilized to reduce the effect of noise. Ideally, Wiener filtering [83] of a large number of previous received values y_k will lead to noise reduction. However, in practice, to extract an accurate fading estimate in the decision-directed mode, adaptive techniques are preferred. In [53, 59], we investigated the effect of various estimation methods on the prediction accuracy for a range of SNR values in conjunction with the TCI adaptive power control method (see Section 2). Due to channel inversion in TCI, the received signal is approximately constant when the predicted power is above the threshold, and the Least Mean Squares (LMS) [83] adaptive tracking is sufficient. The MSE performance comparison that illustrates the noise reduction capability of the adaptive tracking is shown in Figure 6. LMS tracking is very attractive low-to-moderate SNR, but the effective SNR and the MMSE saturate for high SNR. These MSE performance gains translate into the BER advantages and make adaptive prediction feasible for realistic SNR values [52, 53, 59].

As explained above, another source of performance degradation is channel mismatch reflected in inaccurate LP coefficients $\underline{d}$ in (4). Ideally, the computation of these coefficients requires matrix inversion (5) that results in heavy computational loads even for moderate model order p (30~50). We investigated adaptive tracking of the LP coefficients that avoids matrix inversion and greatly reduces channel mismatch [52, 59]. This method is based on updating the estimates of $\underline{d}$ using the LMS algorithm:

$$\underline{d}(n+1) = \underline{d}(n) + \eta e_n \underline{c}_n^* \tag{9}$$

where η is the step-size, $e_n = c_n - \hat{c}_n$, $\underline{c}_n = (c_{n-1}, \cdots, c_{n-p})$. This adaptation is performed iteratively during the observation interval to achieve convergence and greatly reduce the required observation interval length. Moreover, it is used during transmission to track channel variations. For stationary channels (without parameter variation), the steady-state MMSE, J_{ada}, of linear prediction when d_j is tracked using LMS is given by [83]:

$$J_{ada} = J_{min} + \frac{1}{2}\eta J_{min} p(1+\frac{1}{2}N_0) \tag{10}$$

where $N_o/2$ is the variance of noise in the observation samples, and J_{min} is the optimal MMSE (7) of linear prediction. This adaptive tracking technique has near-optimal performance as illustrated in Figure 7 [53].

Utilization of long range prediction in adaptive modulation

This example illustrates the BER gains that can achieved using adaptive modulation when LRP is employed. We consider a fixed power and modulation level-controlled scheme based on square MQAM signal constellations. The target $BER_{tg} = 10^{-3}$ [57]. We restrict the MQAM constellations to sizes M = 0, 2, 4, 16, 64. In the design of an adaptive modulation system, one needs to take into account the accuracy of available CSI. If the modulation rule is designed for perfect CSI, and there are CSI errors, the algorithm will not meet its target BER specifications. In [57], we developed a statistical model for the CSI error of the MMSE channel prediction (eq. (4-6)) that can aid the appropriate modulation level selection. This model produces the probability density function (p.d.f.) $p_\beta(x)$ of the ratio $\beta(t) = \alpha(t) / \hat{\alpha}(t)$, where $\alpha(t) = |c(t)|$ in (2) is the actual fading coefficient, and $\hat{\alpha}(t)$ is its estimate. The design rule for the modulation level selection is as follows: given fixed transmitter power E_s, or the average received SNR per symbol $\bar{\gamma} = E_s/N_0$ (we assume $E(\alpha^2(t))=1$), to maintain a target BER, we need to adjust the modulation size M according to the instantaneous channel gain $\alpha(t)$. In other words, the adaptive modulation scheme can be specified by the threshold values α_i, i = 1, …, 4, defined as: when $\alpha(t) \geq \alpha_i$, M_i-QAM is employed, where $M_1 = 2$, $M_i = 2^{2(i-1)}$, i > 1. When perfect CSI $\alpha(t)$ is available, these thresholds can be directly calculated from the BER bound of MQAM for an AWGN channel [4]: $BER_M \leq 0.2 \exp(-1.5\gamma/(M-1))$ for M>2, and $BER_2 = Q(\sqrt{2\gamma})$, where $\gamma = \alpha^2(t)\bar{\gamma}$ is the instantaneous received SNR. However, when the predicted CSI $\hat{\alpha}(t)$ is used, the appropriate bound BER^*_M, can be obtained by evaluating the expectation of BER_M over $\beta(t)$ using $p_\beta(x)$. The bound BER^*_M should be used to calculate thresholds instead of BER_M when only the predicted CSI is available. (In a related technique in [21], noiseless delayed CSI is assumed available at the transmitter, and the BER^*_M is calculated based on a conditional Rician distribution of the current channel amplitude.) When this selection rule is applied to CSI obtained without the aid of long range prediction, the bit rate gains associated with adaptive modulation are significantly reduced for realistic mobile radio conditions. However, when LRP is applied to standard stationary fading models, there is very small difference between the thresholds calculated using perfect and predicted CSI, even for large vehicle speeds. Thus, in this case, calculation of new threshold values is not required[5]. As a result, *LRP allows adaptive MQAM to achieve its ideal bit rate for realistic mobile radio conditions.*

We examined the BER performance of adaptive modulation aided by channel prediction, and the simulation results are shown in Figure 8. In this figure, we use predicted CSI $\hat{\alpha}(t)$ to select the modulation level, while the thresholds are calculated based on the perfect CSI assumption. We set target

[5] In [85], we showed that the non-stationarity limits the performance of adaptive modulation as the prediction range increases. In this case, the new thresholds need to be recalculated based on BER^*_M to satisfy the target BER. Although this results in reduction of the bit rate relative to the ideal case, the bit rate is still significantly larger than when outdated CSI is used [85].

$BER_{tg} = 10^{-3}$ and assume the modulation switches at the symbol rate of 25Kb/s. Both one-step (2 ms ahead) and five-step (10 ms ahead) prediction were considered in Figure 8. We can see that our long range prediction algorithm provides accurate enough CSI to maintain the target BER using the thresholds calculated based on the perfect CSI. However, when delayed CSI is used, and the thresholds are still calculated based on the perfect CSI (this procedure is called '*static design*' in [21]), the BER performance significantly departs from the target BER even for much more modest delays. Similar conclusions were obtained for a more practical adaptive modulation technique that limits the switching rate [57]. This example, as well as transmission diversity results in Section 2 and truncated channel inversion experiments in section 4 demonstrate that *the LRP algorithm satisfies the required accuracy criteria and provides enabling technology for adaptive transmission.*

4. LONG RANGE PREDICTION FOR REALISTIC PHYSICAL CHANNEL MODEL AND ACTUAL MEASURED DATA

All the simulation results presented above are based on the Jakes model [60] that is often used as a standard simulation model for the Rayleigh fading channel. However, the variation of channel parameters associated with the scatterers (amplitudes, frequencies and phases in (2)) is not captured by this stationary model or by the stationary Rayleigh random process characterization. Thus, in order to test the long-range prediction algorithm and its application in adaptive transmission systems for realistic mobile radio channels, we introduced a novel realistic physical model of the flat fading channel based on the method of images in [54, 58]. This physical model differs from ray-tracing calculations since we are interested in *local* flat fading, not *large-scale* log-normal fading. We showed that more realistic view of the fading signal results from modeling it as a deterministic process formed by the addition of several slowly varying scattered components. Furthermore, we used actual field measurements to validate both the physical model and the performance of our prediction method [55, 58].

Realistic Physical Modeling

Fading of wireless signals is a deterministic process that results from the interference between signals following various paths to the receiver. Although this fact is well known, the implications on the long term channel behavior (that affects the LRP performance) have not been investigated until [54, 58]. In these investigations, we demonstrated two important properties of realistic fading processes that are directly related to the success of the long range prediction.

First, in contrast to the fast variation of the fading signal c(t), *the parameters A_n, f_n and ϕ_n in (2) vary on a much lower time scale*. The rate of change depends on the local environment, so we give a few examples for the carrier frequency of 1 GHz and the vehicle speed of 60 mph. For a mobile 100 meters

from the base station and near a large hill or building, the variation of amplitudes A_n is negligible, and Doppler shifts of all components vary at up to 25 Hz/sec. A challenging case results from passing two meters from a 'spherical' car, for which the Doppler shift of a reflected component can vary at up to 900 Hz/sec, with significant amplitude variation, although still at a rate much slower than that of c(t). Shadowing by a nearby building can also be challenging, resulting in the addition of a significant scatterer in as little as 0.1 sec, although this time increases linearly with the distance from the building. These events (passing closely to a car or shadowing by a nearby building) are short-lived and relatively rare. Insights into these properties can be found in the model based on the method of images combined with diffraction theory as discussed in [58]. *This parameter variation limits the range for which the fading process can be reliably forecasted* given current and past fading measurements. It also determines the required *adaptation speed* for the adaptive tracking method used with the LRP algorithm. The second important conclusion is that the *number of significant scatterers is often modest* even in the indoor environment. (A significant scatterer has power within ~10dB of the power of the strongest component.) Thus, *long range prediction investigations should focus on models with relatively few scatterers*, as well as on Rayleigh fading.

Note that accurate modeling of the number of scatterers and the variation of parameters is not critical in the applications that are concerned with *short term* channel behavior (e.g., channel estimation or short range prediction). The fading autocorrelation functions for different values of N in (2) do not diverge until the delay τ is large (see Fig. 4 and [53]). Similarly, stationary models are sufficient for these applications since parameters do not change significantly over short time intervals. In LRP, the observation interval, the memory span and the prediction range are much larger (see Section 3), so realistic non-stationary modeling is necessary.

The proposed realistic physical model was validated using actual field measurements provided by Ericsson, Inc. These measurements were collected by a van along a route in low density urban Stockholm. During the measurement, the speed of the van varied between 0 and 50 km/h, though mostly at 30km/h or below. The frequency of the radio wave was 1877.5 MHz. The data set contains 100,000 samples of the flat fading signal sampled at the rate of 1562.5Hz. We analyzed this data and found that different portions of the data set had different shapes of the autocorrelation function [58] (here and later in the paper, the empirical autocorrelation function of the observation samples is implied, not the statistical autocorrelation function of a random process) . This was due to the variation in the number and locations of the scatterers along the measurement track. By adjusting the types and positions of the scatterers in our physical model, we were able to match the autocorrelation functions of different data set segments to those produced by the model. These experiments provided us with insights into the nature of flat fading and the impact on the prediction accuracy. For example, one segment of the data set had the

autocorrelation function that resembled that of the Rayleigh fading channel (Figure 4). This autocorrelation shape was obtained using our physical model by placing several curved uniformly distributed scatterers along two sides of the track of the mobile so that the image-sources subtended a large angle from the mobile. Another segment of the measured data had an autocorrelation function with a much wider main lobe and a flatter tail. This autocorrelation function shape was matched by placing several large flat reflectors along the track. The flat objects have distant image sources, so the angle subtended by them is smaller. The same Maximum Doppler shift (eq. (1)) of 46 Hz was used in both experiments. This behavior of the autocorrelation functions can be explained by observing that both the range and the rate of variation of channel parameters (primarily the received Doppler shift range) increase when the image-sources move closer to the mobile, and thus subtend a larger angle from the mobile. The large Doppler shift range makes the channel behave as the Rayleigh fading process associated with small coherence time (see footnote 3) and large sidelobes of the autocorrelation function. However, when the image sources are far from the mobile, the Doppler shift range becomes small (since the variation of the incident angles of radio waves is small). The small subtended angle to the image sources widens the main lobe, while nonstationarity flattens the tail of the autocorrelation function. This causes much larger coherence time for the same maximum Doppler shift (eq. (1)), i.e. the signal samples are correlated for a longer time interval.

This comparison indicates that varied scattering environment needs to be taken into account in designing optimal long range prediction methods. For example, it has been verified that the large memory span is very important for accurate long range prediction in the Rayleigh fading channel (the first model). Its utility in the second model depends on the balance between the prediction range and the distance over which the nonstationarity washes out the sidelobes of the autocorrelation function.

Adaptive long range prediction for non-stationary data

As discussed above, in a realistic non-stationary mobile radio environment, the Doppler shifts and other parameters associated with the scatterered components in (2) slowly vary. The poles of the AR model in (4) are primarily determined by these Doppler shifts [49]. Since the LP coefficients $\underline{d}$ in (5) directly depend on these poles, we need to update the $\underline{d}$-vector continuously to keep up with these variations. For most typical cases, the scattering parameters vary slowly enough to be captured by standard adaptive techniques [54, 58]. In the following results, the LMS algorithm was employed in the tracking of the LP coefficients as in eq. (9). Adaptation for prediction more than one step ahead is presented in [54, 59].

To test the LRP method on the waveforms generated by the physical channel model, an interference pattern was generated over an area of 10×10 meters, using one large flat and five curved (spherical) reflectors along one side [54]. The Maximum Doppler frequency shift was assumed to be 90 Hz. We

compared the performance of channel *power* prediction for a *typical* case (car drives parallel to and ~10m from five close image sources) and a *challenging* case (car drives towards the reflectors (10 to 0 meters)). The power prediction absolute error comparison is shown in Figure 9a. We observe that the channel power variation can be predicted very closely for a typical situation. However, the prediction becomes more difficult for the challenging case due to large Doppler frequency shift and large power variation as the mobile approaches the reflectors [54, 58]. Many experiments were performed for this and other interference patterns, and it was concluded that reliable prediction for most cases can be achieved for prediction ranges of about half a wavelength or less. When the prediction range approaches a wavelength, prediction accuracy decreases. In addition, we compared the MSE performance vs prediction range for a *stationary* Jakes model and two non-stationary fading data sets: the physical data and the measured data in Figure 9b. All data sets correspond to the case when the image sources subtend a large angle from the mobile (see the discussion on realistic physical modeling above). Thus, the empirical autocorrelation functions of all data sets resembled Fig. 4, with the Doppler shift of 46 Hz. Despite the similarity of the autocorrorelation functions, the MSE for the Jakes model is much lower than for two other data sets. This significant MSE gain is due to stationarity. Moreover, the prediction capability of the stationary Jakes model dataset is improved by a lower sampling rate. This agrees with our previous analysis in section 3. However, the prediction for the non-stationary measured and physical model data is not improved significantly by the lower sampling rate (not shown). This comparison shows that the prediction capability of LRP is limited by the parameter variation in realistic fading environments. Thus, on one hand, a non-stationary model such as that described here is necessary to test prediction algorithms, and, on other hand, other techniques need to be explored to increase prediction range further. Exploration of nonlinear methods and comparison with the techniques in the literature (e.g. [41, 42]) is one of our future research directions.

The long range prediction method was also tested on measured data [55, 58]. Numerous tests using various segments of the data set demonstrated that long range prediction is feasible for this channel. In addition, the LRP for measured data was combined with adaptive modulation and truncated channel inversion algorithm in [55, 57, 58]. As an example, simulation results for the segment of the data with the measured correlation function similar to that of the Rayleigh fading (Fig. 4) for the TCI scheme are shown in Figure 10. Note significant performance gain of the LRP (with prediction) relative to the case when the outdated channel coefficients are used to adjust the transmitter power for data bits between the two adjacent low rate samples (without prediction). As we increase the prediction range in this experiment, prediction accuracy deteriorates faster than for a data set generated by the Jakes model, despite the similarity in the average autocorrelation functions of the two waveforms. As for the physical model

above, this can be explained by the non-stationarity of measured data that results from parameter variation.

5. CONCLUSION

We demonstrated that accurate long range channel prediction is essential for reliable adaptive transmission over fading mobile radio channels. Theoretical and simulation results in this paper utilize standard fading models, a novel non-stationary physical model and measurement data to validate the proposed LRP algorithm. While long range prediction is clearly a promising tool when utilized jointly with adaptive transmission in realistic wireless applications, many exciting theoretical, experimental and practical problems need to be addressed in the future to realize its potential.

ACKNOWLEDGEMENT

The authors would like to thank Jan-Eric Berg and Henrik Asplund of Ericsson, Inc. for providing the measurement data set. We would also like to thank Tugay Eyceoz and Secin Guncavdi for helpful discussions.

REFERENCES

1. M. Zeng, A. Annamalai, and V. K. Bhargava, "Recent Advances in Cellular Wireless Communications," *IEEE Commun. Mag.*, Vol. 37, No. 9, Sept. 1999, pp. 128 - 138.
2. M. W. Oliphant, "The Mobile Phone Meets the Internet," *IEEE Spectrum*, Vol. 36, No. 8, Aug. 1999, pp. 20 – 28.
3. A. J. Goldsmith and S. G. Chua, "Adaptive Coded Modulation for Fading Channels," *IEEE Trans. Commun.*, Vol. 46, No. 5, May 1998, pp. 595 - 601.
4. A. J. Goldsmith and S. G. Chua, "Variable-Rate Variable-Power MQAM for Fading Channels," *IEEE Trans. Commun.*, Vol. 45, No. 10, Oct. 1997, pp. 1218 - 1230.
5. M. S. Alouini, X. Tang, and A. J. Goldsmith, "An Adaptive Modulation Scheme for Simultaneous Voice and Data Transmission over Fading Channels," *IEEE J. Select. Areas. Commun.*, Vol. 17, No. 5, May 1999, pp. 837 – 850.
6. A. J. Goldsmith and P. Varaiya, "Capacity of Fading Channels with Channel Side Information," *IEEE Trans. Inform. Theory*, Vol. 43, No. 6, Nov. 1997, pp. 1986 – 1992.
7. M. S. Alouini, and A. J. Goldsmith, "Capacity of Rayleigh Fading Channels Under Different Adaptive Transmission and Diversity-Combining Techniques," *IEEE Trans. Veh. Technol.*, Vol. 48, No. 4, July 1999, pp. 1165 – 1181.
8. K. Arimochi, S. Sampei, N. Morinaga, "Adaptive Modulation System with Discrete Power Control and Predistortion-Type Nonlinear Compensation for High Spectral Efficient and High Power Efficient Wireless Communication Systems," *Proc. IEEE Int. Symp. on Personal, Indoor and Mobile Radio Commun., PIMRC'97*, Vol. 2, 1997, pp. 472 – 476.
9. S. Otsuki, S. Sampei, and N. Morinaga, "Square-QAM Adaptive Modulation / TDMA / TDD Systems Using Modulation Level Estimation with Walsh Function," *Electron. Lett.*, Vol. 31, No. 3, Feb. 1995, pp. 169 – 171.
10. T. Ue, S. Sampei, and N. Morinaga, "Symbol Rate and Modulation Level Controlled Adaptive Modulation System with TDMA/TDD for High Bit Rate Transmission in High Delay Spread Environments," *Electron. Lett.*, Vol. 32, No. 4, Feb. 1996, pp. 304 – 305.
11. S. Otsuki, S. Sampei, and N. Morinaga, "Modulation Level Controlled Adaptive Modulation System with Base-Station-Based Transmission/Reception Diversity Scheme for Personal Communications," *IEEE GLOBECOM'95*, Vol. 2, 1995, pp. 1537 – 1541.
12. W. T. Webb and R. Steele, "Variable Rate QAM for Mobile Radio," *IEEE Trans. Commun.,* Vol. 43, No. 7, July 1995, pp. 2223 – 2230.
13. J. M. Torrance and L. Hanzo, "Optimisation of Switching Levels for Adaptive Modulation in Slow Rayleigh Fading," *Electron. Lett.*, Vol. 32, No. 13, June 1996, pp. 1167 – 1169.

14. M. Torrance, D. Didascalou, and L. Hanzo, "The Potential and Limitations of Adaptive Modulation Over Slow Rayleigh Fading Channels," *IEE Colloquim on the future of Mobile Multimedia Commun.*, 1996, pp. 10/1 – 10/6.
15. J. M. Torrance and L. Hanzo, "Upper Bound Performance of Adaptive Modulation in a Slow Rayleigh Fading Channel," *Electron. Lett.*, Vol. 32, No. 8, April 1996, pp. 718 – 719.
16. J. Williams, L. Hanzo, and R. Steele, "Channel-Adaptive Modulation," *IEE Radio Receivers and Associated Systems*, 26 – 28 Sept. 1995, pp. 144 – 147.
17. J. M. Torrance and L. Hanzo, "Demodulation Level Selection in Adaptive Modulation," *Electron. Lett.*, Vol. 32, No. 19, Sept. 1996, pp. 1751 – 1752.
18. J. M. Torrance and L. Hanzo, "Adaptive Modulation in a Slow Rayleigh Fading Channel," *Proc. of PIMRC'96*, Vol. 2, 1996, pp. 497 – 501.
19. J. M. Torrance and L. Hanzo, "Latency and Networking Aspects of Adaptive Modems over Slow Indoor Rayleigh Fading Channels, " *IEEE Trans. Veh. Technol.*, Vol. 48, No. 4, July 1999, pp. 1237 – 1251.
20. L. Hanzo, "Bandwidth-Efficient Wireless Multimedia Communications," *Proceedings of the IEEE*, Vol. 86, No. 7, July 1998, Vol. 86, No. 7, pp. 1342 – 1382.
21. D. L. Goeckel, "Adaptive Coding for Fading Channels Using Outdated Channel Estimates," *Proc. IEEE Veh. Technol. Conf., VTC'98,* Vol. 3, 1998, pp. 1925 - 1929.
22. D. L. Goeckel, "Strongly Robust Adaptive Signaling for Time-Varying Channels," *Proc. IEEE Int. Commun. Conf., ICC'98,* Vol. 1, 1998, pp. 454 - 458.
23. B. Vucetic, "An Adaptive Coding Scheme for Time-Varying Channels," *IEEE Trans. Commun.*, Vol. 39, No. 5, May 1991, pp. 653 – 663.
24. R. Chen, K. C. Chua, B. T. Tan, and C. S. Ng, "Adaptive Error Coding Using Channel Prediction," *Proc. IEEE Int. Symp. on Personal, Indoor and Mobile Radio Commun., PIMRC'96*, 1996, pp. 359 – 363.
25. B. Narendran, J. Sienicki, S. Yajnik, and P. Agrawal, "Evaluation of an Adaptive Power and Error Control Algorithm for Wireless Sytems," *Proc. IEEE Int. Commun. Conf., ICC'97*, Vol. 1, 1997, pp. 349 – 355.
26. P. Agrawal, B. Narendran, J. Sienicki, and S. Yajnik, "An Adaptive Power Control and Coding Scheme for Mobile Radio Systems," *Proc. IEEE Int. Conf. on Personal Wireless Commun., ICPWC'96*, pp. 283 – 288.
27. V. K. N. Lau, and S. V. Maric, "Variable Rate Adaptive Channel Coding for Coherent and Non-coherent Rayleigh Fading Channel," *Proc. IEEE Int. Conf. on Personal Wireless Commun., ICPWC'97*, pp. 75 – 79.
28. V. K. N. Lau, and M. D. Macleod, "Variable Rate Adaptive Trellis Coded QAM for High Bandwidth Efficiency Application in Rayleigh Fading Channels," *Proc. IEEE Veh. Technol. Conf., VTC'98*, Vol. 1, 1998, pp. 348 – 352.
29. V. K. N. Lau, and S. V. Maric, "Variable Rate Adaptive Modulation for DS-CDMA," *IEEE Trans. Commun.*, Vol. 47, No. 4, April 1999, pp. 577 – 589.
30. V. K. N. Lau, "Channel Capacity and Error Exponents of Variable Rate Adaptive Channel Coding for Rayleigh Fading Channels," *IEEE Trans. Commun.*, Vol. 47, No. 9, Sept. 1999, pp. 1345 – 1356.
31. D. Cygan and E. Lutz, "A Concatenated Two-Stage Adaptive (CTSA) Error Control Scheme for Data Transmission in Time-Varying Channels," *IEEE Trans. Commun.*, Vol. 43, No. 2/3/4, Feb./March/April 1995, pp. 795 – 803.
32. K. Rohani, M. Harrison, and K. Kuchi, "A Comparison of Base Station Transmit Diversity Methods for Third Generation Cellular Standards," *Proc. IEEE Veh. Technol. Conf., VTC'99*, Vol. 1, 1999, pp. 351 – 355.
33. M. Raitola, A. Hottinen and R. Wichman, "Transmission Diversity in Wideband CDMA," *Proc. IEEE Veh. Technol. Conf., VTC'99*; Vol. 2, July 1999, pp. 1545 – 1549.
34. T. K. Yo, "Maximum Ratio Transmission," *IEEE Trans. Commun.*, Vol. 47, No. 10, Oct. 1999, pp. 1458 – 1461.
35. D. Rajan, S. D. Gray, "Transmit Diversity Schemes for CDMA-2000," *Proc. of IEEE Wireless Commun. and Networking Conf. WCNC'99*, Vol. 2, 1999, pp. 669 – 673.
36. A. Hottinen, and R. Wichman, "Transmit Diversity by Antenna Selection in CDMA Downlink," *Proc. of 1998 IEEE 5th International Symposium on Spread Spectrum Techniques and Applications*, pp. 767 – 770.
37. C. Chien, M. B. Srivastava, R. Jain, P. Lettieri, V. Aggarwal, and R. Sternowski, "Adaptive Radio for Multimedia Wireless Links," *IEEE J. Select. Areas. Commun.*, Vol. 17, No. 5, May 1999, pp. 793 – 813.
38. S. Abeta, S. Sampei, and N. Morinaga, "Adaptive Coding Rate and Process Gain Control with Channel Activation for Multi-Media DS/CDMA Systems," *IEICE Trans. Commun.* Vol. E80-B, No. 4, April 1997.
39. A. S. Amanullah, and M. Salehi, "Adaptive Quantization for Fading Channels with Feedback," *Int. Journal of Wireless Inform. Networks*, Vol. 2, No. 2, 1995, pp. 83 – 89.
40. T. Ojanpera, and R. Prasad, *Wideband CDMA for Third generation Mobile Communications*. Artech House, 1998.
41. J. B. Andersen, J. Jensen, S. H. Jensen, and F. Frederiksen, "Prediction of Future Fading Based on Past Measurements," *Proc. IEEE Veh. Technol. Conf., VTC'99*, Sept. 1999.
42. T. Ekman, and G. Kubin, "Nonlinear Prediction of Mobile Radio Channels: Measurements and MARS Model Design," *Proc. IEEE ICASSP'99*, Vol. 5, 1999, pp. 2667 – 2670.
43. J. K. Hwang, and J. H. Winters, "Sinusoidal Modeling and Prediction of Fast Fading Processes," *IEEE GLOBECOM'98*, pp. 892 – 897.
44. X. M. Gao, M. A. Tanskanen, and S. J. Ovaska, "Comparison of Linear and Neural Network Based Power Prediction Schemes for Mobile DS/CDMA Systems," *Proc. IEEE Veh. Technol. Conf., VTC'96*, May 1996, pp. 61 – 65.

45. Y. S. Zhang, and D. B. Li, "Volterra Adaptive Prediction of Multipath Fading Channel," *Electron. Lett.,* Vol. 33, No. 9, April. 1997, pp. 754 – 755.
46. C. Spillard, G. J. R. Povey, "Application of the Prony Algorithm to a Predictive RAKE Receiver," *Proc. of IEEE 4th International Symposium on Spread Spectrum Tech, and applications*, Vol. 3, 1996, pp. 1039 - 1042.
47. Q. Shen, B. X. Wu, and A. K. Elhakeem, "The Linear Prediction Method of Fading Channel Estimation for the RAKE Receiver with Impulsive Interference", *Wireless Personal Communications*, vol. 6, 1998, pp. 233 - 248.
48. H. S. Wang and P. C. Chang, "On Verifying the First-Order Markovian Assuption for a Rayleigh fading Channel Model," *IEEE Trans. Veh. Technol.*, Vol. 45, No. 2, May 1996, pp. 353 – 357.
49. T. Eyceoz, A. Duel-Hallen, H. Hallen, "Prediction of Fast Fading Parameters by Resolving the Interference Pattern," *Proceeding of ASILOMAR conference on signal and systems,* Vol. 1, 1997, pp. 167 - 171.
50. T. Eyceoz, A. Duel-Hallen, H. Hallen, "Using the Physics of the Fast Fading to Improve Performance for Mobile Radio Channels," *Proc. IEEE Int. Symp. On Inform. Theory, ISIT'98,* pp. 159.
51. T. Eyceoz, A. Duel-Hallen, H. Hallen, "Deterministic Channel Modeling and Long Range Prediction of Fast Fading Mobile Radio Channels," *IEEE Commun. Lett.,* Vol. 2, No. 9, Sept. 1998, pp. 254 – 256.
52. T. Eyceoz, S. Hu, A. Duel-Hallen, H. Hallen, "Adaptive Prediction, Tracking and Power Adjustment for Frequency Non-Selective Fast Fading Channels," *Proc. the Commun. Theory Mini-Conference*, *ICC'99*, June 1999, pp.1 - 5.
53. T. Eyceoz, S. Hu, and A. Duel-Hallen, "Performance Analysis of Long Range Prediction for Fast Fading Channels," *Proc. of 33rd Annual Conf. on Inform. Sciences and Systems CISS'99*, March 1999, Vol. II, pp. 656 - 661.
54. S. Hu, H. Hallen and A. Duel-Hallen, "Physical Channel Modeling, Adaptive Prediction and Transmitter Diversity for Flat Fading Mobile Channels," *Proc. IEEE Workshop on Signal Processing Advances in Wireless Commun., SPAWC'99*, May 1999, pp.387 - 390.
55. S. Hu, H. Hallen and A. Duel-Hallen, "Adaptive Power Control Using Long Range Prediction for Realistic Fast Fading Channel Models and Measured Data", *5th International Symposium on Communication Theory and Application ISCTA'99*, July 1999, pp. 118 - 120.
56. S. Hu, T. Eyceoz, A. Duel-Hallen, H. Hallen, "Transmitter Antenna Diversity and Adaptive Signaling Using Long Range Prediction For fast fading DS/CDMA Mobile radio Channels," *Proc. of IEEE Wireless Commun. and Networking Conf. WCNC'99*, Vol. 2, 1999, pp. 824 – 828.
57. S. Hu, A. Duel-Hallen, H. Hallen, "Adaptive Modulation using Long Range Prediction for Fast Flat Fading Channels," submitted to *IEEE Int. Symp. On Inform. Theory, ISIT'2000*.
58. S. Hu, H. Hallen, and A. Duel-Hallen, "Physical Models for Understanding and Testing Long Range Prediction of Flat Fading in Wireless Communication," to be submitted to *IEEE J. Select. Areas. Commun.*
59. S. Hu, T. Eyceoz, A. Duel-Hallen, H. Hallen, "Adaptive Long Range Prediction for Rapidly Varying Flat Fading Channels with Applications to Mobile Radio Systems," to be submitted to *IEEE Trans. Commun.*
60. W.C. Jakes, *Microwave Mobile Communications*. Wiley, New York, 1974.
61. J.G. Proakis, *Digital Communications*. Third Edition, McGraw-Hill, 1995.
62. E. Biglieri, G. Cairo, and G. Taricco, "Coding and Modulation under Power Constraints", *IEEE Personal Communications*, Vol. 5, No. 3, June 1998, pp. 32 - 39.
63. B. Sklar, "Rayleigh Fading Channels in Mobile Digital Communication Systems, Part 1: Characterization," *IEEE Commun. Mag.*, Vol. 35, No. 7, July 1997, pp. 90 – 100.
64. S. Stein, "Fading Channel Issues in System Engineering," *IEEE J. Select. Areas. Commun.*, Vol. 5, No. 2, Feb. 1987, pp. 68 - 69.
65. T.S. Rappaport, *Wireless Communications: Principles and Practice*. Prentice-Hall, 1996.
66. R. C. V. Macario, *Cellular Radio*. 2nd Edition, McGraw Hill, 1997.
67. W. T. Webb, and L. Hanzo, *Quadrature Amplitude Modulation: Principles and Applications for Fixed and Wireless Channels*. Pentech Press, 1994.
68. S. Sampei, *Applications of Digital Wireless Techniques to Global Wireless Communications*. PTR, 1997.
69. J. K. Cavers, "Variable-Rate Transmission for Raleigh Fading Channels," *IEEE Trans. Commun.*, Vol. 20, No. 1, Feb. 1972, pp. 15 – 22.
70. J. F. Hayes, "Adaptive Feedback Communications," *IEEE Trans. Commun.*, Vol. 16, No. 1, Feb. 1968, pp. 29 – 34.
71. V. O. Hentinen, "Error Performance for Adaptive Transmission on Fading Channels," *IEEE Trans. Commun.*, Vol. 22, No. 9, Sept. 1974, pp. 1331 – 1337.
72. G. D. Forney, L. Brown, M. V. Eyuboglu, J. L. Moran III, "The V.34 High-Speed Modem Standard," *IEEE Commun. Mag.*, Dec. 1996, pp. 28 – 33.
73. S. K. Lai, R. S. Cheng, K. B. Letaief, and R. D. Murch, "Adaptive Trellis Coded MQAM and Power Optimization for OFDM Transmission," *Proc. IEEE Veh. Technol. Conf., VTC'99*, Vol. 1, pp. 290 – 294..
74. X. Qiu, and K. Chawla, "On the performance of Adaptive Modulation in Cellular Systems," *IEEE Trans. Commun.* Vol. 47, No. 6, June 1999, pp. 884 – 894.
75. M. Filip, and E. Vilar, "Implementation of Adaptive Modulation as a Fade Countermeasure," *Int. Journal of Satellite Commun.*, Vol. 12, 1994, pp. 181 – 191.
76. M. Zorzi and R. R. Rao, "Energy-Constrained Error Control for Wireless Channels," *IEEE Personal Communications*, Vol. 4, No. 6, Dec. 1997, pp. 27 – 33.

77. M. B. Pursley, and C. S. Wilkins, "Adaptive-Rate Coding for Frequency-Hop Communications over Rayleigh Fading Channels," *IEEE J. Select. Areas. Commun.*, Vol. 17, No.7, July 1999, pp. 1224 – 1231.
78. S. M. Alamouti, and S. Kallel, "Adaptive Trellis-Coded Multiple-Phase-Shift Keying for Rayleigh Fading Channels," *IEEE Trans. Commun.*, Vol. 42, No. 6, June 1994, pp. 2305 – 2314.
79. J. M. Jacobsmeyer, "Adaptive Trellis-Coded Modulation for Bandlimited Metor Burst Channels," *IEEE J. Select. Areas. Commun.*, Vol. 10, No.3, April 1992, pp. 550 – 561.
80. K. Balachandran, S. R. Kadaba, and S. Nanda, "Channel Quality Estimation and Rate Adaptation for Cellular Mobile Radio," *IEEE J. Select. Areas. Commun.*, Vol. 17, No.7, July 1999, pp. 1244 – 1256.
81. E. Dahlman *et al.*, "WCDMA – The Radio Interface for Future Mobile Multimedia Communications," *IEEE Trans. Veh. Technol.*, vol. 47, No. 4, Nov. 1998, pp. 1105 – 1117.
82. F. Adachi, M. Sawahashi, and H. Suda, "Wideband DS-CDMA for Next Generation Mobile Communications Systems," *IEEE Commun. Mag.*, Sept. 1998, pp. 56 – 69.
83. M.H. Hayes, *Statistical Digital Signal Processing and Modeling*. John Wiley & Sons, Inc., 1996.
84. G. B. Giannakis, C. Tepedelenlioglu, "Basis Expansion Models and Diversity Techniques for Blind Equation of Time-Varying Channels," Proceedings of the IEEE, Vol. 86, pp. 1969-1986, Oct. 1998.
85. S. Hu, A. Duel-Hallen, H. Hallen, "Long Range Prediction Makes Adaptive Modulation Feasible for Realistic Mobile Radio Channels," submitted to *Proc. of 34rd Annual Conf. on Inform. Sciences and Systems CISS'2000*.
86 M. K. Tsatsanis and G. B. Giannakis, "Modeling and Equalization of Rapidly Fading Channels," *Int. J. Adaptive Control and Signal Processing*, vol. 10, no. 2/3, pp. 159-176, March 1996.
87 M. K. Tsatsanis and G. B. Giannakis, "Equalization of Rapidly Fading Channels: Self-recovering Methods," *IEEE Trans. Commun.*, vol. 44, no. 5, pp. 619-630, May 1996.
88 L. Lindbom, "Adaptive Equalization for Fading Mobile Radio Channels," M.S. Thesis, Uppsala University, Sweden, 1992.

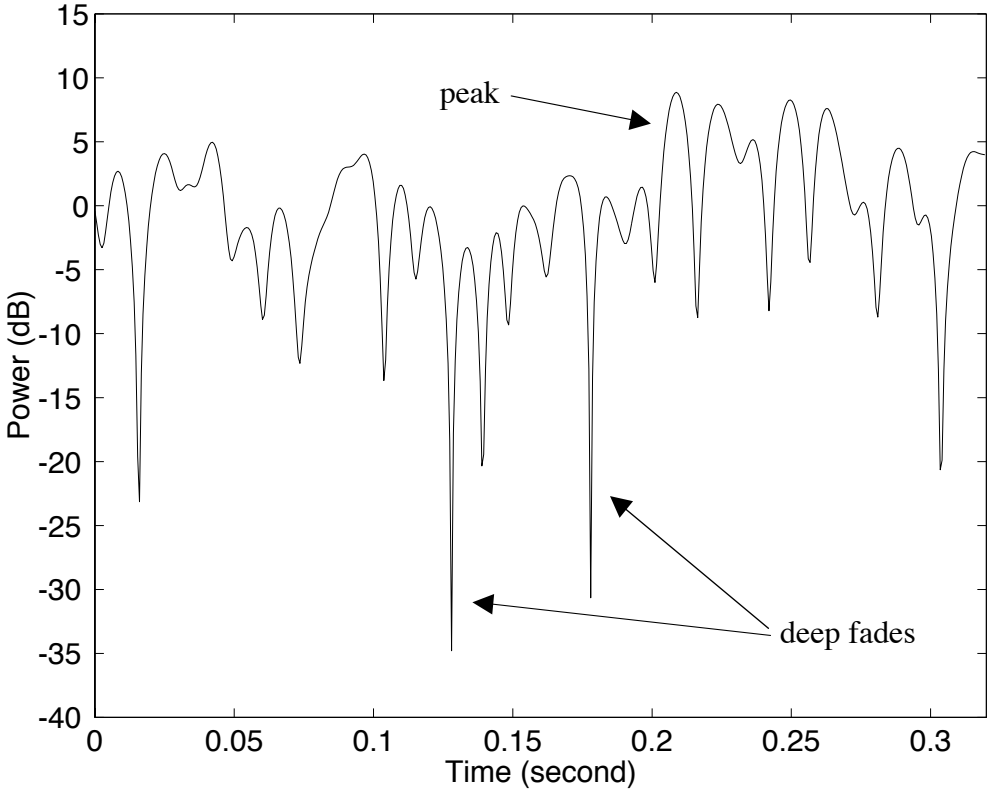

Figure 1. A typical fading signal (Provided by Ericsson, Inc.)

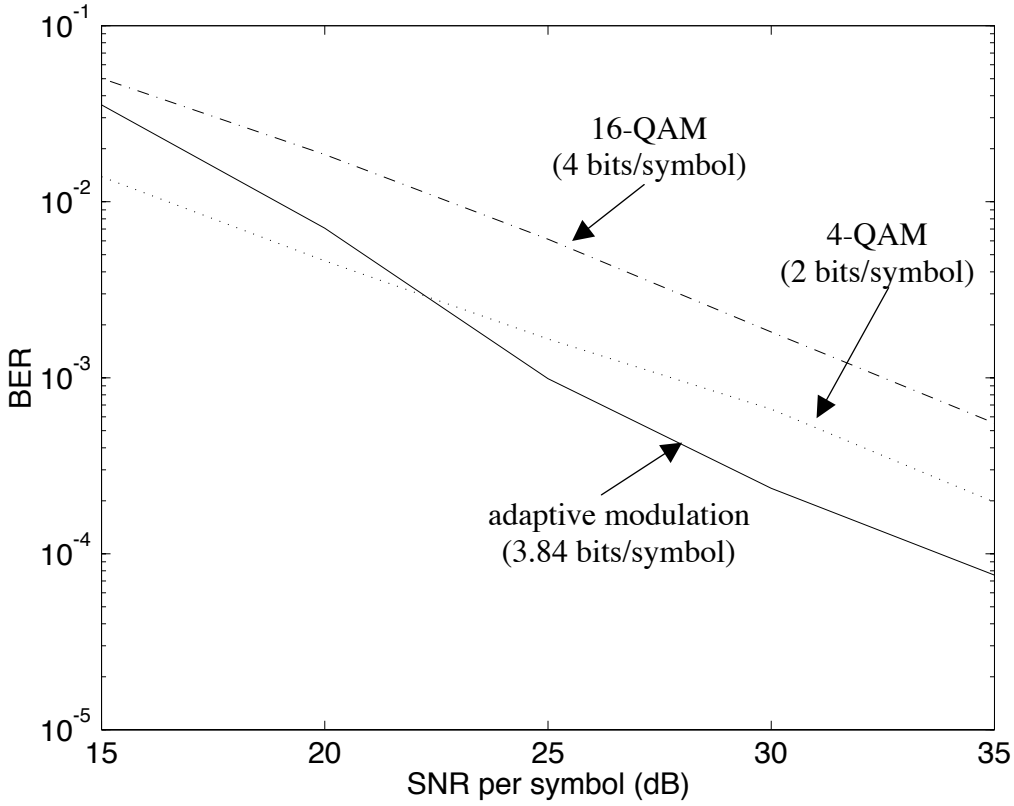

Figure 2. Using adaptive modulation to exploit the potential of the Rayleigh fading channel.

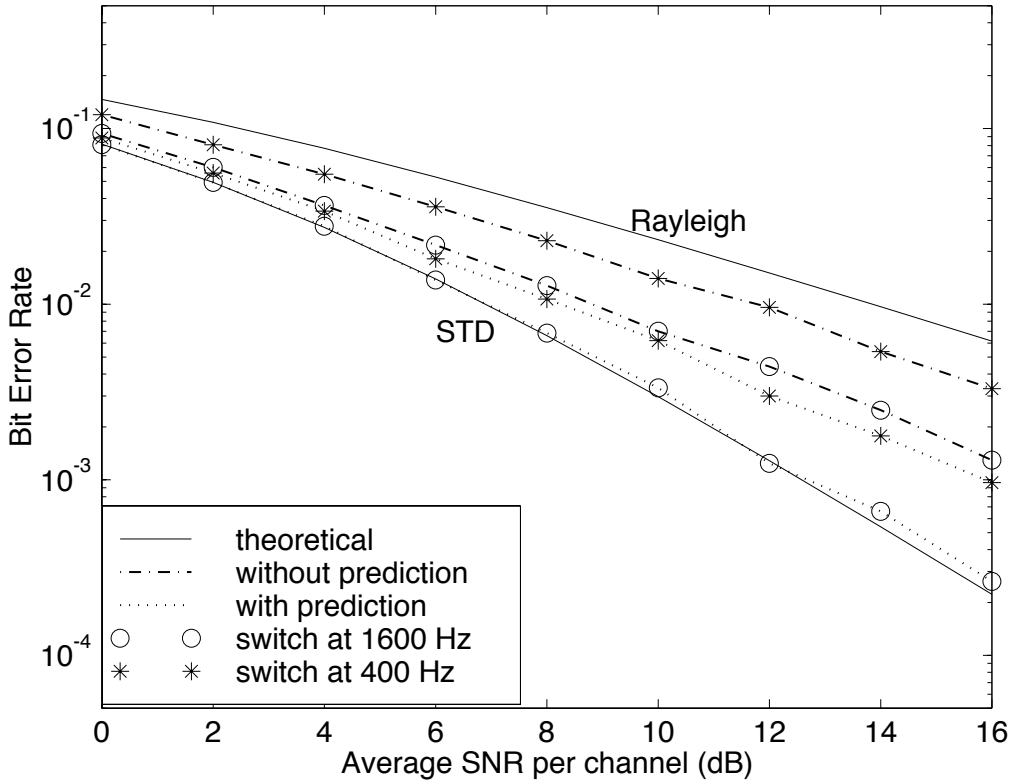

Figure 3. Performance improvement of Selection Transmitter diversity system using long-range channel prediction. Maximum Doppler shift 200Hz.

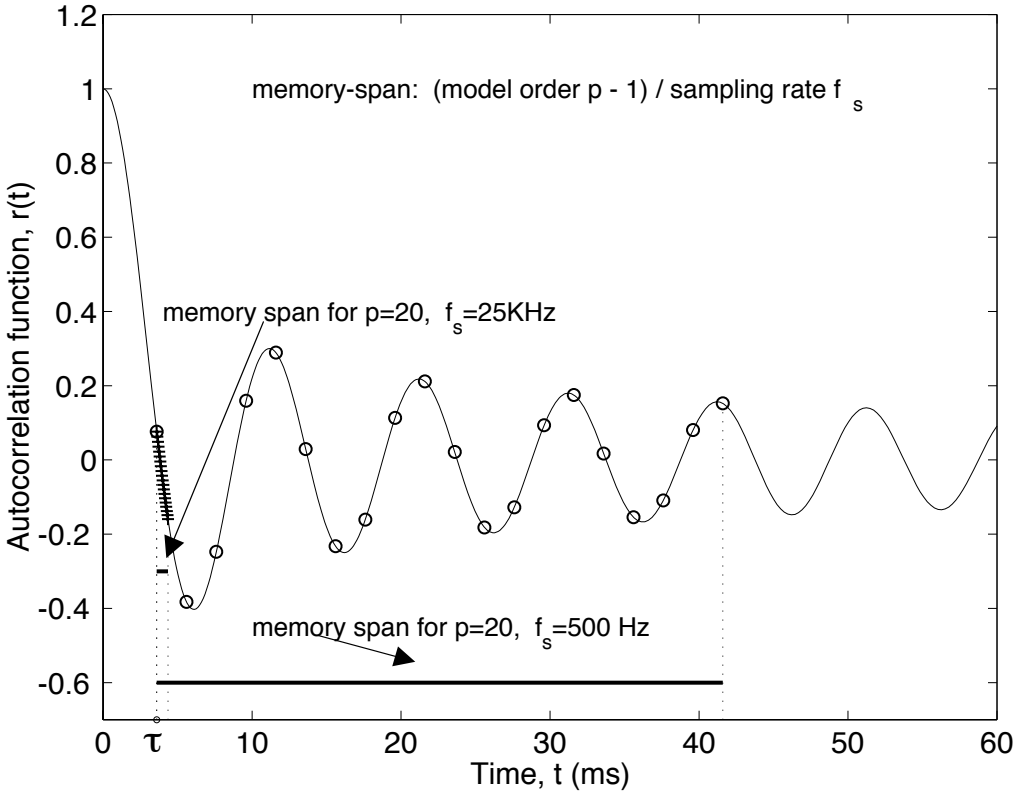

Figure 4. Theoretical autocorrelation function of the Rayleigh fading channel and the memory span of the MMSE prediction. Maximum Doppler shift 100Hz.

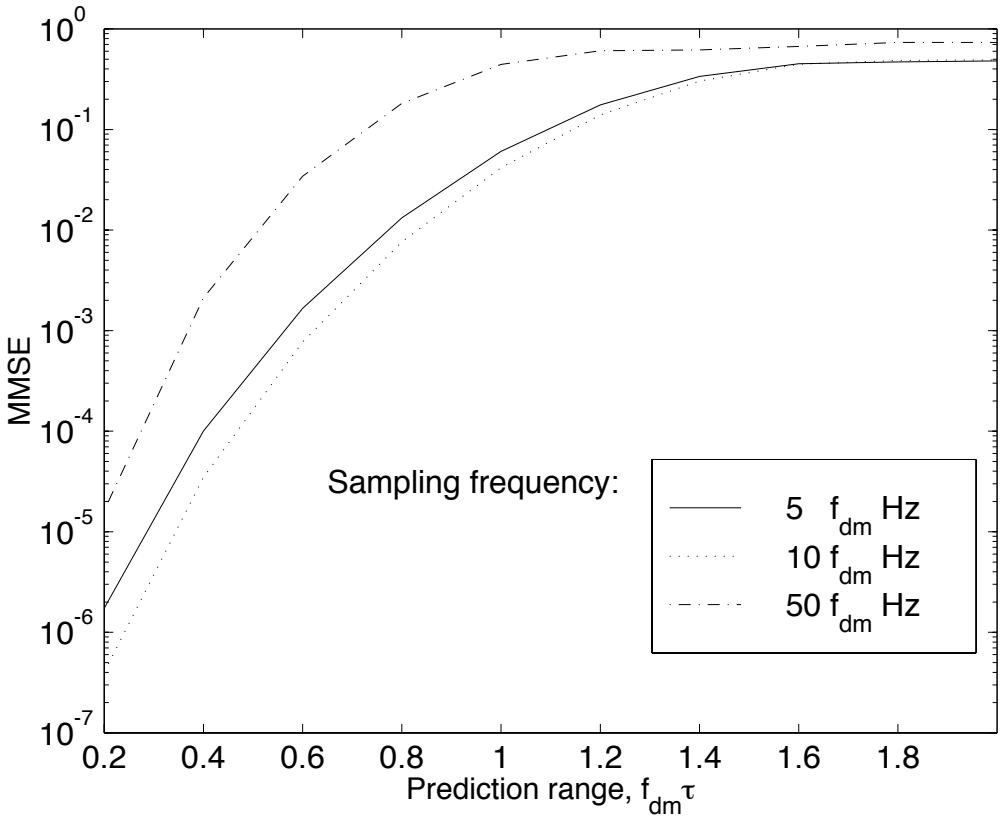

Figure 5. The MMSE for the long range prediction for different values of sampling rate, f_s, with model order p=50, and SNR = 100 dB. Rayleigh fading channel.

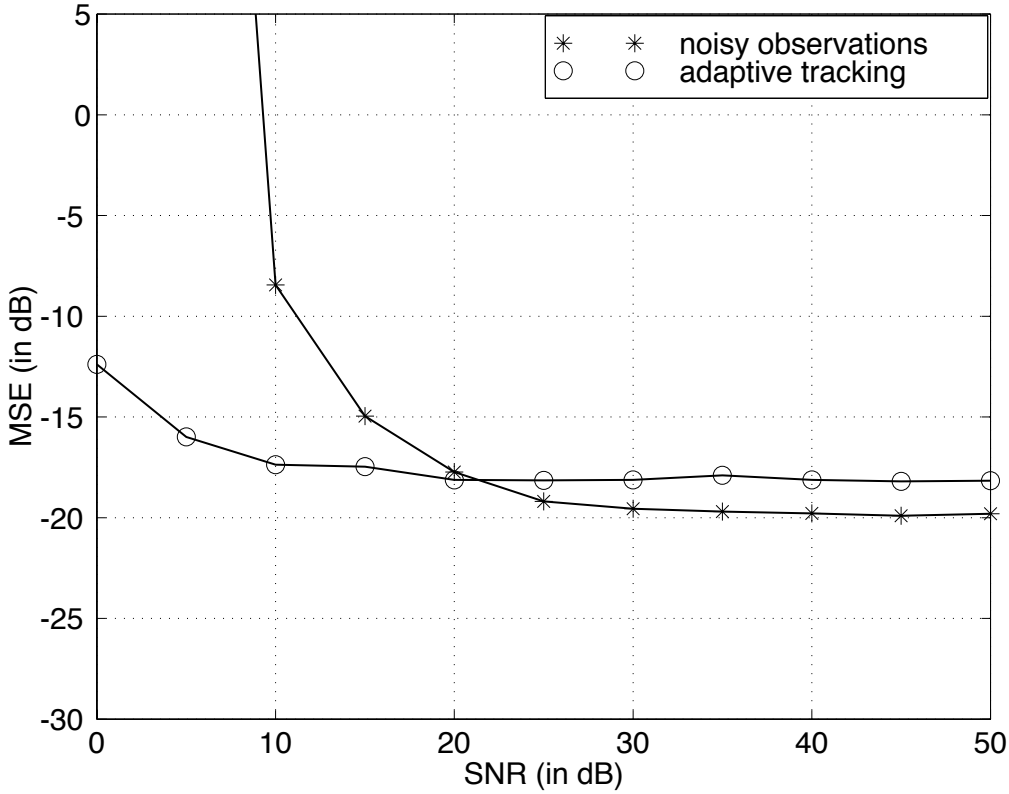

Figure 6. Prediction MSE performance comparison with and without adaptive tracking of received signal coefficient for the TCI algorithm. Maximum Doppler shift 100Hz.

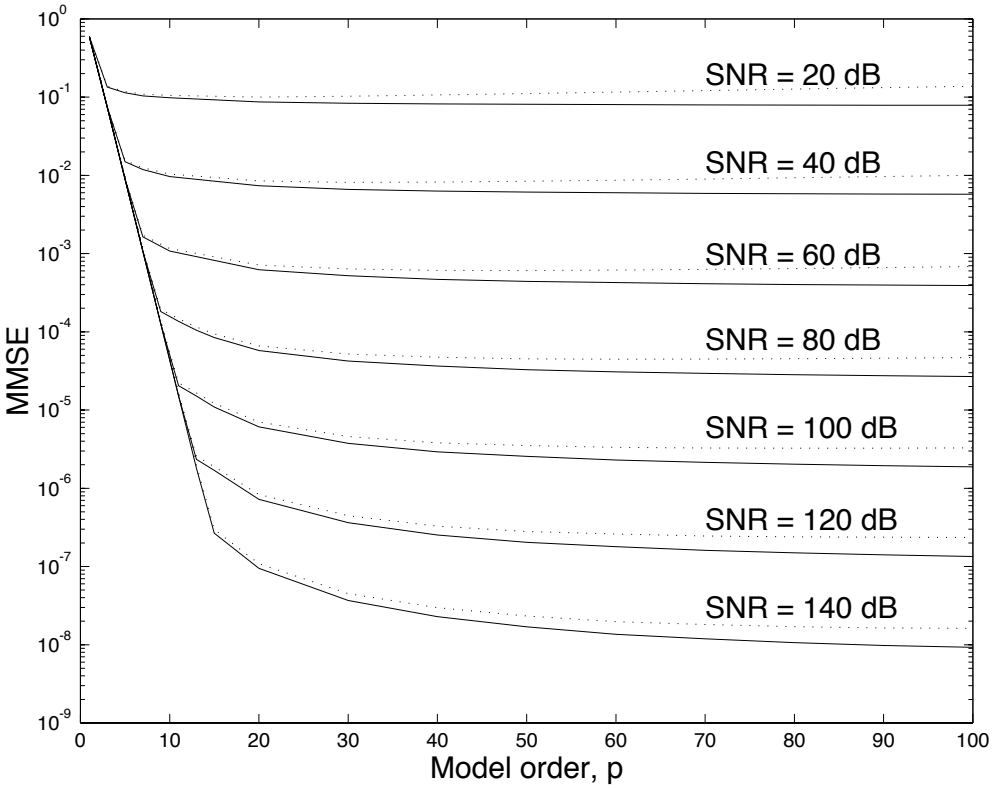

Figure 7. MMSE vs. model order, p, for different values of SNR for the sampling rate of 500 Hz, τ = 2ms, f_{dm}=100Hz. Solid lines: optimal; Dotted lines: adaptive tracking of linear prediction coefficients. Raleigh fading channel.

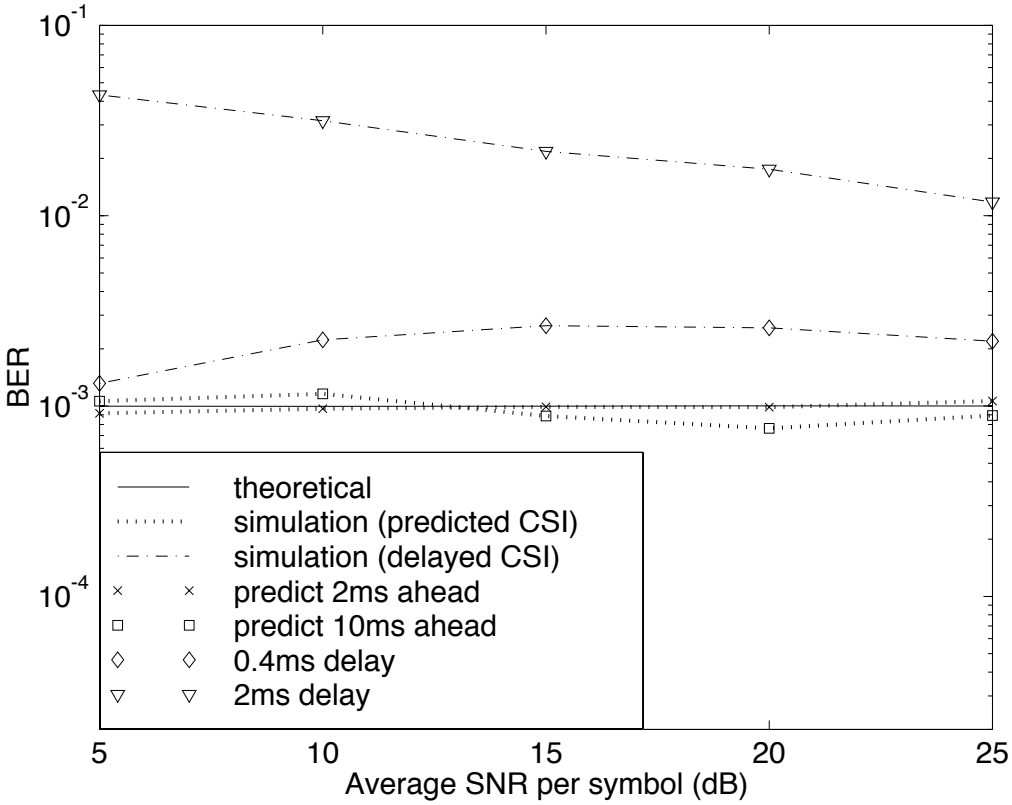

Figure 8. BER performance gains of adaptive modulation with and without LRP. Maximum Doppler shift 100Hz.

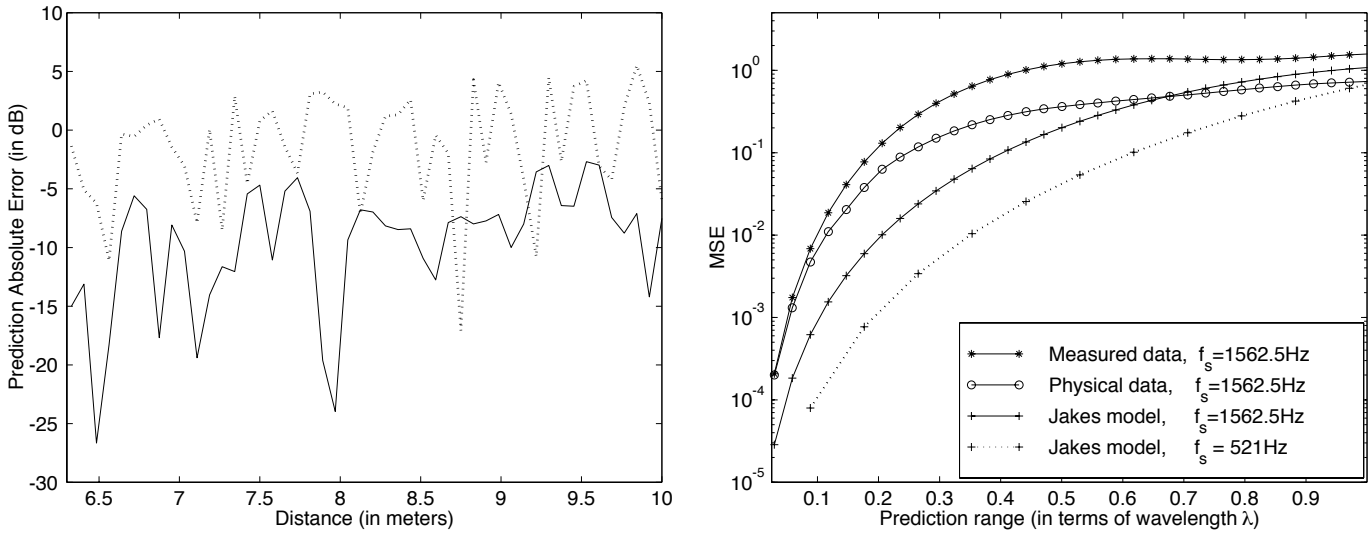

Figure 9. (a) Power prediction absolute error comparison for realistic fading model. Solid: typical case; Dotted: challenging case. Prediction range 2.92 ms (0.26 λ). Maximum Doppler shift 90 Hz. (b) Prediction mean square error as a function of the prediction range for stationary data (Jakes model) and non-stationary data (physical model and measurements). p = 40, Maximum Doppler shift 46 Hz.

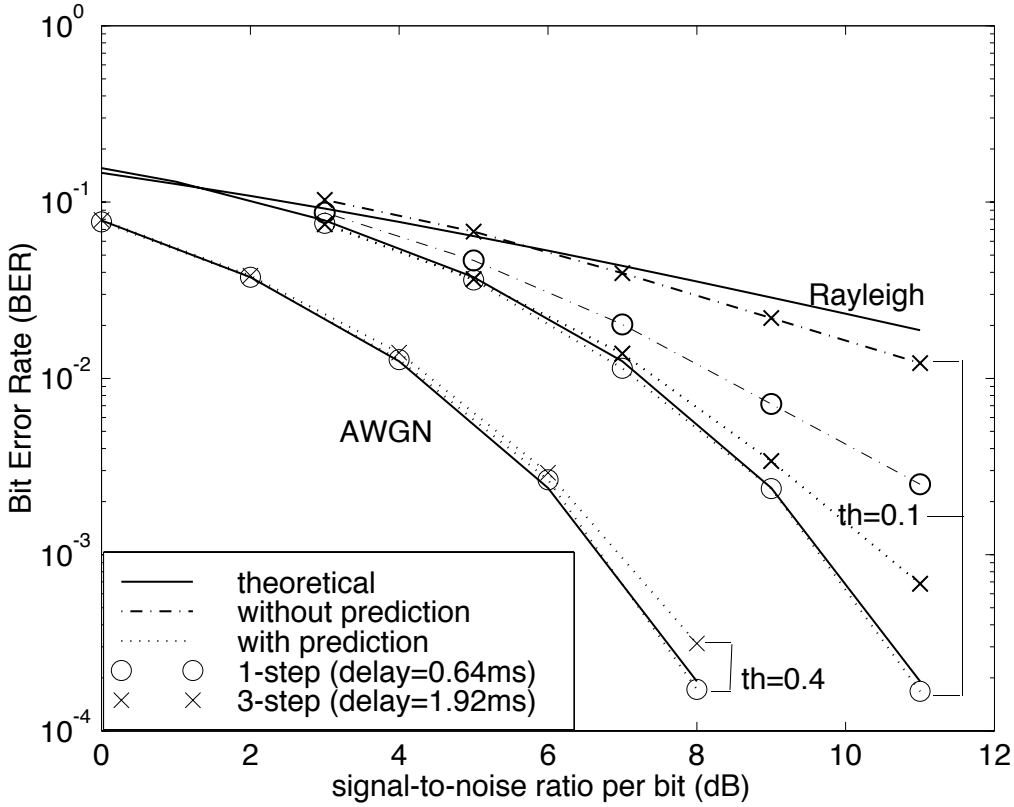

Figure 10. Performance gains of LRP for truncated channel inversion over measured data set.